NUCLEAR THEORY, Vol. 37 (2018)
eds. M. Gaidarov, N. Minkov, Heron Press, Sofia

Tensor Force Effect on the Structure Evolution in Si Isotopes

M.R. Oudih, **M. Ouhachi**, **M. Fellah**, **N.H. Allal**

Laboratoire de Physique Théorique, Faculté de Physique, USTHB
BP 32, El Alia, 16111 Bab Ezzouar, Algiers, Algeria

Abstract. The tensor force effect on the nuclear structure properties for Si isotopes is studied within the self-consistent Hartree-Fock-Bogoliubov approach. The Skyrme energy density functional has been considered in the particle-hole channel, while the zero range delta-interaction has been employed in the particle-particle channel. In order to correctly treat the pairing correlation, particle-number projection was carried out by the Lipkin-Nogami method. Rotational correction as approximate angular momentum projection is also introduced in order to restore the rotational symmetry. The bulk properties like binding energy, two-neutron separation energy and charge radius are thus investigated with and without tensor force and compared with recent experimental data. To study the tensor effect on the shape evolution, the potential energy curves are displayed and discussed.

1 Introduction

The tensor force is an important and necessary ingredient of the nucleon-nucleon interaction and has a crucial influence on the nuclear structure. It was originally included as part of Skyrme effective zero-range nucleon-nucleon interaction, 60 years ago [1]. However, it has been neglected in the fitting process of most mean-field forces due to its complexity. In the last decade, this force has received renewed interest due to its very specific effect on nuclear spectra [2, 3]. It brings a correction to binding energies and to spin-orbit splitting that fluctuates with the filling of shells. Its introduction seems, therefore, necessary to improve the predictive power of mean-field-based methods. The purpose of this work is the investigation of the tensor force effect on the structure of Si isotopes. The Hartree-Fock-Bogoliubov theory is employed with three different Skyrme interactions, namely, SLy4, SLy5 and SLy5T [4, 5].

2 Formalism

The HFB approximation can be derived using the variational principle starting from an effective Hamiltonian given as:

$$H = \sum_{ij} t_{ij} a_i^\dagger a_j + \frac{1}{4} \sum_{ijkl} v_{ijkl} a_i^\dagger a_j^\dagger a_l a_k, \tag{1}$$

where $a_i^\dagger$ and a_i are the creation and annihilation operators of a particle in the state $|i\rangle$. t_{ij} and v_{ijkl} are respectively the matrix elements of the kinetic energy operator and an antisymmetrized matrix elements of the effective nucleon-nucleon interaction. The ground-state wave function is considered to be the vacuum of quasiparticles:

$$\alpha_i |\Psi\rangle = 0, \forall i \tag{2}$$

defined by the canonical Bogoliubov transformation [6]:

$$\begin{pmatrix} \alpha \\ \alpha^\dagger \end{pmatrix} = \begin{pmatrix} U^\dagger & V^\dagger \\ V^T & U^T \end{pmatrix} \begin{pmatrix} a \\ a^\dagger \end{pmatrix}. \tag{3}$$

The ground state energy can be expressed in terms of the density matrix

$$\rho_{ij} = \langle\Psi| a_j^\dagger a_i |\Psi\rangle, \tag{4}$$

and the pairing tensor

$$\kappa_{ij} = \langle\Psi| a_j a_i |\Psi\rangle, \tag{5}$$

as [7, 8]:

$$E(\rho,\kappa) = \sum_{ij}(t_{ij} - \lambda)\rho_{ji} + \frac{1}{2}\sum_{ijlm} v_{ijlm}\rho_{li}\rho_{mj} + \frac{1}{4}\sum_{ijlm} v_{ijlm}\kappa_{lm}\kappa^*_{ij}. \tag{6}$$

The HFB equations are obtained by minimizing the ground-state energy with respect to ρ and κ:

$$\begin{pmatrix} h-\lambda & \Delta \\ -\Delta^* & -h^*+\lambda \end{pmatrix} \begin{pmatrix} U_k \\ V_k \end{pmatrix} = E_k \begin{pmatrix} U_k \\ V_k \end{pmatrix}, \tag{7}$$

where E_k are the quasiparticle energies and λ is the chemical potential introduced as a Lagrange multiplier to ensure an average particle-number conservation. h and Δ, respectively, denote the mean-field Hamiltonian and pairing potential.

As it is known, the deformed Hartree-Fock-Bogoliubov procedure destroys the assumed particle-number, translational and rotational invariance of the wave-function. In order to restore the particle-number symmetry, the Lipkin-Nogami (LN) prescription has been considered [9–11]. The latter is an efficient method to approximately restore the particle-number before the variation. The LN equations are obtained by replacing the HFB energy (6) with $E[\rho,\tilde{\rho}] - \lambda_2 \left\langle \Delta\hat{N}^2 \right\rangle$, where $\left\langle \Delta\hat{N}^2 \right\rangle = \left[\hat{N} - \left\langle \hat{N} \right\rangle\right]^2$ and λ_2 is a coefficient that depends on the HFB wave-function. In practice, the LN method is implemented by only a slight modification of the pairing-field and the Hartree-Fock potential according to Ref. [12].

In the case of translation symmetry, we considered the simplest method which consists in introducing the factor $(1 - 1/A)$ in the kinetic energy density

expression as an approximate center-of-mass correction. The energy correction from angular-momentum projection in the Gaussian-Overlap-Approximation (GOA) for axially symmetric nuclei is given by: $-\Delta J_y^2/2I$, where I is the moment of inertia [8]. This energy gain is due to the fluctuation of the angular momentum which causes a zero point rotation.

For the Skyrme interaction the total energy of a nucleus is expressed as the volume integral. It can be modeled by an energy density functional that is the sum of five terms:

$$\mathcal{H}(\mathbf{r}) = \mathcal{H}_{Kin}(\mathbf{r}) + \mathcal{H}_{Sk}(\mathbf{r}) + \mathcal{H}_{Coul}(\mathbf{r}) + \mathcal{H}_{Pair}(\mathbf{r}) + \mathcal{H}_{corr}. \quad (8)$$

The first term corresponds to the kinetic energy density. Assuming time-reversal symmetry, the Skyrme energy density functional $\mathcal{H}_{Sk}$ takes the form: [13, 14]

$$\mathcal{H}_{Sk} = \sum_{t=0,1} C_t^{\rho}\,\rho_t^2 + C_t^{\Delta\rho}\,\rho_t\,\Delta\rho_t + C_t^{\tau}\,\rho_t\,\tau_t + C_t^{J}J_t^2 + C_t^{\nabla J}\rho_t\nabla\cdot\mathbf{J}_t, \quad (9)$$

where t stands for the isoscalar ($t = 0$) or isovector ($t = 1$) channel. The definitions of the various densities ρ_t, τ_t, and $\mathbf{J}_t$, for each channel, can be found in Refs. [15–17]. The coefficients $C_t^{\rho} = C_{t0}^{\rho} + C_{tD}^{\rho}\rho_0^{\gamma}$ are isoscalar density dependent while all the others are real constants [18].

$\mathcal{H}_{Coul}(\mathbf{r})$ is the Coulomb energy density involved for protons. This term contains the direct and exchange contributions. While the former is treated exactly, the Slater approximation is adopted for the exchange Coulomb energy [15]:

$$\mathcal{H}_{Coul}(\mathbf{r}) = \frac{e^2}{2}\rho_p(\mathbf{r})\int d^3\mathbf{r}'\frac{\rho_p(\mathbf{r}')}{|\mathbf{r}-\mathbf{r}'|} - \frac{3}{4}e^2\left(\frac{3}{\pi}\right)^{\frac{1}{3}}\rho_p^{\frac{4}{3}}(\mathbf{r}). \quad (10)$$

$\mathcal{H}_{Pair}(\mathbf{r})$ is the pairing energy density which reads:

$$\mathcal{H}_{Pair}(\mathbf{r}) = \sum_q \frac{V_0^q}{2}\left(1 - \frac{1}{2}\frac{\rho_0(\mathbf{r})}{\rho_c}\right)\tilde{\rho}^2(\mathbf{r}), \quad (11)$$

where V_0^q ($q = n, p$) is the pairing strength, $\rho_c = 0.16\,\mathrm{fm}^{-3}$ is the saturation density and $\tilde{\rho}(\mathbf{r})$ is the local pairing density [19].

$\mathcal{H}_{Corr}$ is the sum of the correction terms derived from the restoration of the broken symmetries.

3 Results and Discussion

As mentioned above, the Skyrme parameterizations SLy4, SLy5 and SLy5T have been used to study the effect of the tensor force. While SLy4 does not contain a tensor term, SLy5 includes the tensor term derived from the central part of the Skyrme interaction. The SLy5T interaction, on the other hand, contains the pure tensor term. In this interaction, the tensor force is added perturbatively to the Skyrme SLy5 interaction by keeping its parameters unchanged.

3.1 Binding energy

In Figure 1, the calculated binding energies per nucleon of Si isotopes in the three Skyrme parameterizations are shown in comparison with the available experimental values of the new version of the Atomic Mass Evaluation AME16 [20]. One can see from the figure that all the curves show a rapid decrease around a maximum obtained at the neutron number $N = 16$ which corresponds to the most stable nucleus of the isotopic chain. It clearly appears that all the effective interactions overestimate the binding energy along the isotopic chain. Moreover, it is found that the SLy4 and SLy5 results are very similar while the inclusion of the tensor term by the SLy5T interaction has the effect of increasing the binding energy. The possible improvement of the agreement between the theoretical binding energies and the experiment when the tensor term is included in a Skyrme interaction has been discussed in several works. While in some works it has been established that the binding energy is not greatly affected by the tensor force, it has been shown in others that this force increases the deviation from the experiment. This may be due to the fact that the mass is among the quantities which are adjusted in the fit [21].

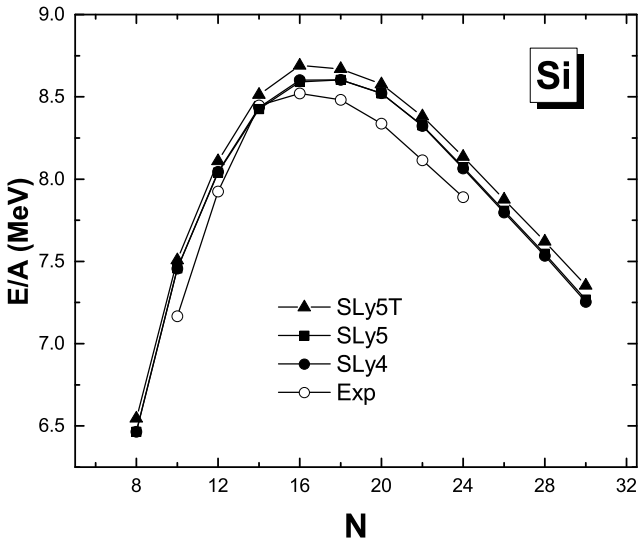

Figure 1. Binding energies per nucleon of Si isotopes as a function of the neutron number.

3.2 Two-neutron separation energy

Two-neutron separation energy is among the physical quantities indicating a change in the structure of the nucleus. This quantity has been computed using the obtained ground-state binding energies for Si isotopes. The calculated two-neutron separation energies, with the SLy4, SLy5 and SLy5T interactions

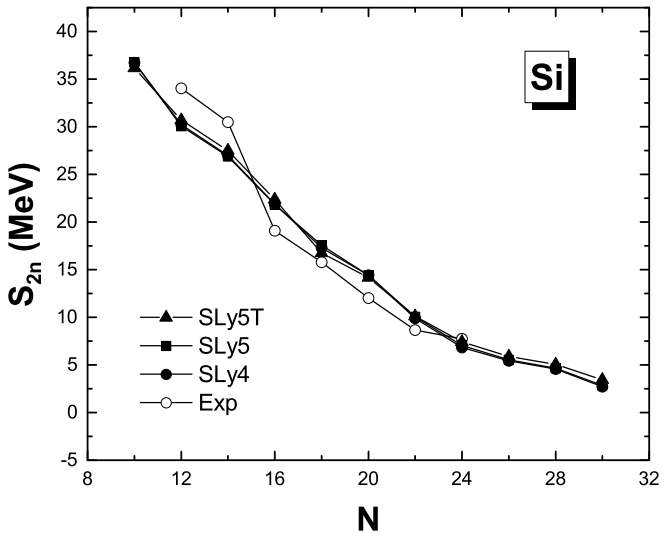

Figure 2. Two-neutron separation energy of Si isotopes as a function of the neutron number.

are compared with the available experimental data in Figure 2. From the Figure it is seen that the theoretical results are in quite good agreement with the experimental data when available. In general, a large fall in the separation energy is observed at magic numbers. Except at $N = 14$, where an abrupt decrease in the S_{2n} value is evident, which indicates a neutron shell closure, the curves do not show any sudden fall of the two neutron separation energies. This indicates that there is no dramatic change in the isotope structure, and in particular a weak shell closure effect at $N = 20$ and 28.

3.3 Root-mean-square charge radii

The evolution of nuclear charge radii along isotopic chains reflects how the mean-field of the protons changes when neutrons are added in the system. A comparison of the calculated charge radii with measurements is displayed in Figure 3. It appears that the interactions with tensor terms (SLy5T) give better descriptions than the interactions SLy4 and SLy5 without the pure tensor term. Indeed, one can see that if the tensor force is switched off, the deviation becomes more important in the direction of larger radii values. On the other hand, the theoretical curves show a parabolic shape typical of a shell closure around $N = 14$. By increasing the number of neutrons, the charge radii increase up to $N = 28$ where we observe a kink which is a sign of sudden change of deformation.

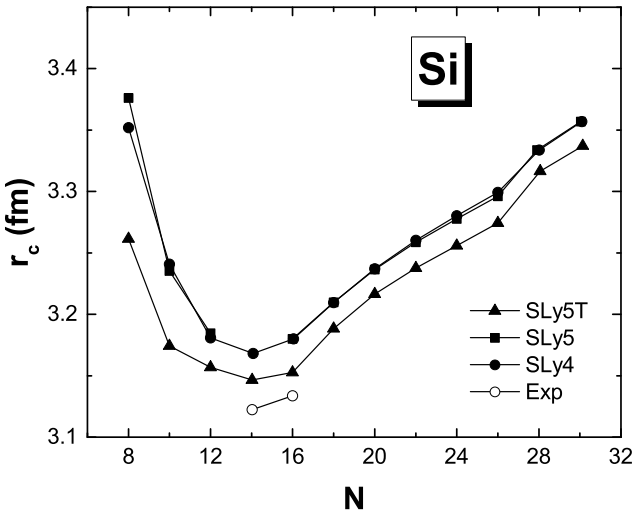

Figure 3. Root-mean-square charge radii of Si isotopes as a function of the neutron number.

3.4 Deformation

In order to investigate the shape evolution of silicon isotopes, the calculated quadruple deformations have been listed in Table 1 for SLy4, SLy5 and SLy5T interaction, respectively. We note that the nuclear shapes obtained with the three interactions are nearly the same. All parameterizations predict a spherical shape

Table 1. Quadrupole deformation parameter of Si isotopes calculated for SLy4, SLy5 and SLy5T interactions.

	β		
Nucleus	SLy4	SLy5	SLy5T
^{22}Si	0.000	0.006	0.000
^{24}Si	0.000	0.000	0.092
^{26}Si	0.243	0.241	0.241
^{28}Si	-0.141	-0.142	-0.107
^{30}Si	0.000	0.000	0.000
^{32}Si	0.000	0.000	0.000
^{34}Si	0.000	0.000	0.000
^{36}Si	0.000	0.000	0.000
^{38}Si	0.000	0.000	0.000
^{40}Si	0.237	0.235	0.117
^{42}Si	-0.143	-0.145	-0.127
^{44}Si	-0.134	-0.134	-0.100

for ^{22}Si and ^{24}Si, a sudden transition to prolate shape at ^{26}Si followed by an abrupt change at ^{28}Si from the prolate to the oblate shape. This scenario repeats itself from ^{28}Si to ^{44}Si: a spherical shape is predicted for ^{30}Si to ^{38}Si, a prolate shape for ^{40}Si, and an oblate shape for ^{42}Si and ^{44}Si. This indicates that the $N = 28$ shell closure disappears due to the deformation effect. The spherical shape at ^{22}Si and ^{34}Si is expected because of the neutron closed shells $N = 8$ and $N = 20$. The same spherical shape might be also expected in ^{24}Si and around ^{34}Si because two or four neutrons outside of the $N = 8$ and $N = 20$ closed shells is not enough to make a deformation. The shape of ^{28}Si and ^{42}Si is explained in some works by the fact that the tensor force has a large effect in nuclei deepening the energy surfaces at oblate energy minima in these nuclei.

Thus the curves of the quadrupole deformation parameter show shape change while no change appears on the curve of the two-neutron separation energy. This could be an indication of shape coexistence, so that a dramatic change in nuclear shape is accompanied by a small change in nuclear binding energy.

3.5 Potential-energy curve

To get more insight into the shapes of Si isotopes, we have plotted in Figure 4 the binding energy curves as a function of quadrupole deformation parameter as obtained with constrained HFB calculations for the different Skyrme interactions. From the figure, where the energy of the spherical shape is taken as reference, we can see that the SLy4 and SLy5 curves are very similar which means that the contribution of tensor force, resulting from the central term of the Skyrme interaction, is not important for any quadrupole deformation value. On the other hand, one notices that the shape of the nuclei progressively evolves from a spherical shape for ^{34}Si to a soft shape with the appearance of a second minimum for $^{40-42}$Si. One then expects a shape coexistence in this region. When the tensor force is added to the SLy5 interaction, the energy curves of the $^{40-42}$Si nuclei become flat: the ground-state minimum becomes less pronounced and the shape

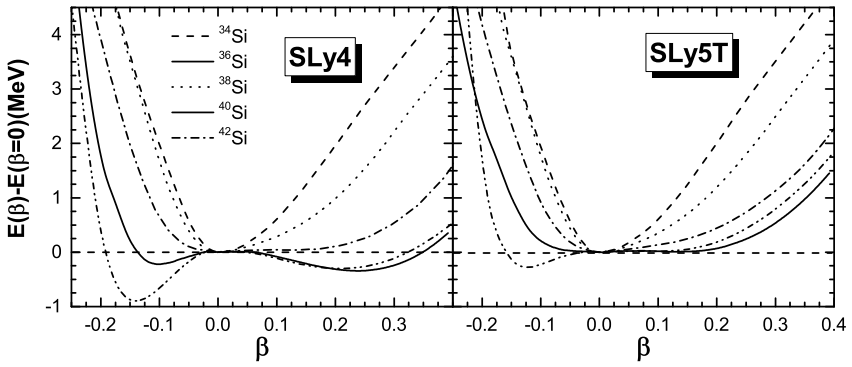

Figure 4. Potential-energy curve of Si isotopes as a function of the neutron number.

coexistence disappears completely since there is no minimal energy in the prolate side. The behavior of the potential energy for ^{40}Si and ^{42}Si indicates that the triaxial degree of freedom may play an important role in the description of the studied nuclei.

4 Conclusion

In conclusion, we have analyzed the tensor force effect on the structure of even-even Si isotopes by a Skyrme-HFB model. The different symmetries broken in the mean-field level have been approximately restored. In the calculation, we have chosen three different Skyrme interactions: SLy4 without tensor interaction, SLy5 (with tensor correlation derived from the central term), and SLy5T (with the pure tensor term). Starting from the proton-rich nuclei up to the neutron-rich side, we have calculated binding energies per nucleon, two-neutron separation energies, rms charge radii, and quadrupole deformations. The available experimental data are globally rather well reproduced. The similarity between the SLy4 and SLy5 results shows that the tensor term derived from the central term of the Skyrme interaction does not play an important role for all the studied nuclei, and can therefore be neglected. It is found that the inclusion of tensor correlation added to the SLy5 force leads to modifications to the total binding energy and rms charge radius. All the considered interactions show that the $N = 28$ spherical shell closure is significantly weakened in Si nuclei. The investigation of the potential energy curves suggests that the inclusion of the triaxial degree of freedom may be required for more reliable predictions.

References

[1] T.H.R. Skyrme, *Phil. Mag.* **1** (1956) 1043.

[2] T. Otsuka, T. Matsuo, and D. Abe, *Phys. Rev. Lett.*, **97**(2006) 162501.

[3] T. Lesinski, M. Bender, K. Bennaceur, T. Duguet, and J. Meyer, *Phys. Rev. C*, **76** (2007) 014312.

[4] E. Chabanat, P. Bonche, P. Haensel, J. Meyer, R. Schaeffer, *Nucl. Phys.* **A635** (1998) 231.

[5] G. Colo, H. Sagawa, S. Fracasso, P.F. Bortignon, *Phys. Lett. B* **646** (2007) 227.

[6] N.N. Bogoliubov, *Sov. Phys. JETP* **7** (1961) 41.

[7] P. Ring, P. Schuck, *The Nuclear Many-Body Problem* (Springer-Verlag, Berlin, 1980).

[8] M. Bender, P.-H. Heenen, P.-G. Reinhard, *Rev. Mod. Phys.* **75** (2003) 121.

[9] H.C. Pradhan, Y. Nogami, J. Law , *Nucl. Phys. A* **201** (1973) 357.

[10] M. Anguiano, J.L. Egido, and L.M. Robledo, *Phys. Lett. B* **545** (2002) 62.

[11] M.R. Oudih, M. Fellah, N.H. Allal, and N. Benhamouda, *Phys. Rev. C* **76** (2007) 047307.

[12] M.V. Stoitsov, J. Dobaczewski, W. Nazarewicz, S. Pittel, and D.J. Dean, *Phys. Rev. C* **68** (2003) 054312.

[13] N. Schunck, J. Dobaczewski, J. McDonnell, J. Moré, W. Nazarewicz, J. Sarich, and M. V. Stoitsov, *Phys. Rev. C* **81** (2010) 024316.

[14] W. Ryssens, P-H. Heenen, and M. Bender, *Phys. Rev. C* **92** (2015) 064318.

[15] M. Bender, P-H. Heenen, and P-G. Reinhard, *Rev. Mod. Phys.* **75** (2003) 121.

[16] J. Dobaczewski, J. Dudek, S.G. Rohoziński, and T.R. Werner, *Phys. Rev. C* **62** (2000) 014310.

[17] T. Lesinski, M. Bender, K. Bennaceur, T. Duguet, and J. Meyer, *Phys. Rev. C* **76** (2007) 014312.

[18] M. Kortelainen, J. McDonnell, W. Nazarewicz, P-G. Reinhard, J. Sarich, N. Schunck, M.V. Stoitsov, and S.M. Wild, *Phys. Rev. C* **85** (2012) 024304.

[19] J. Dobaczewski, H. Flocard, and J. Treiner, *Nucl. Phys. A* **422** (1984) 103.

[20] M. Wang, G. Audi, F. G. Kondev, W. J. Huang, S.Naimi, and Xing Xu, *Chin. Phys. C* **41** (2017) 030003 .

[21] M. Ouhachi, M.R. Oudih, M. Fellah, N.H. Allal, *Chin. J. Phys.* **56** (2018) 574.